

Modeling the effects of non-ideal ankle exoskeleton controllers on assisted standing balance in older adults with impaired muscle strength

Daphna Raz¹, Necmiye Ozay¹, and Brian R. Umberger²

Abstract—Ankle exoskeletons can compensate for plantar flexion and dorsiflexion torque deficits that commonly occur with aging by providing assistive torque at the ankle joint. This added torque assistance may be particularly useful for improving stability during standing. However, studies have shown that ankle exoskeletons may both enhance and hinder standing balance, particularly in weaker older adults. Furthermore, the ideal amount and timing of ankle exoskeleton assistance for an older adult is not known. Here, we examine the effects of exoskeleton strength, controller parameter uncertainty, and actuation delay on a simple model of a frail older female. We compute the set of body center of mass (CoM) positions and velocities from which it is possible for the model to maintain standing balance with a minimally assistive exoskeleton, a moderately assistive exoskeleton, and a strongly assistive exoskeleton. We also explore the effect of errors in model-dependent exoskeleton controller parameters including imprecise estimation of the CoM location. Lastly, we incorporate state feedback delay in the exoskeleton controller, including delay that is synchronized with the biological rate of torque development in the model. We find that a stronger exoskeleton is not necessarily better, with a moderately strong exoskeleton improving stability the most. CoM uncertainty has a smaller, but still meaningful effect, reducing feasible stability in low-velocity standing sway conditions that are common in daily life. Stability at such nominal conditions is most affected by exoskeleton delay, with feasible stability decreasing exponentially as delay grows.

Clinical relevance As they become more commonplace, the responsibility for prescribing, adjusting, and tuning exoskeletons will at least partially fall to clinicians.

I. INTRODUCTION

Humans maintain standing balance via postural adjustments that can range from subtle shifts in the center of pressure (CoP) [1] to taking a step [2] or grabbing onto external supports. Control of ankle torque is an important strategy that is used to shift the CoP under the foot to maintain stability, particularly in response to small to medium perturbations [2]. These perturbations may be external forces or ‘internal’ miscalculations due to factors such as sensorimotor noise

While the ankle strategy is used throughout the lifespan, functional joint-level changes occur at the ankle during aging that may negatively affect stability. In particular, the maximum available plantar and dorsiflexion torques are significantly lower in older adults, as is the rate at which this

torque can be produced [3]. These constrained and slower torque production dynamics can lead to reduced performance on standing balance tasks [4], [5] and greater fall risk [6]. In particular, older adults living in long-term care facilities frequently experience falls during standing [7], possibly due to this population having a high rate of frailty [8].

Ankle exoskeletons, which are powered orthotic devices designed to increase torque capacity, have the potential to mitigate the loss of ankle strength that typically occurs with aging, thereby improving stability. However, their effect on standing balance has only recently been explored, with mixed results. Ankle exoskeletons have been found to improve [9], hinder [10], and have little effect [11] on stability during standing, depending on the perturbation paradigm and assumptions on the exoskeleton control strategy. Notably, these studies considered only able-bodied young adults.

In our recent work, we have modeled the effect of ankle exoskeleton assistance on standing balance in younger and older adults [12]. We developed a generalizable method to compute the set of feasible body center of mass (CoM) positions and velocities from which it is possible to maintain standing balance [13]. We call this set the ‘stabilizable region.’ We extended this method and used it to compute stabilizable regions for sex- and age- adjusted models of standing balance, both with and without ankle exoskeleton assistance [12]. We showed that gravity compensation and proportional-derivative control, which are commonly used exoskeleton controller strategies, may slightly reduce feasible stability in younger adults relative to their unassisted baseline. In older adults, the effect is more nuanced. While an ankle exoskeleton may increase stability at low CoM sway velocities, especially by increasing the range of statically stable positions over the foot, it acts as a disturbance at higher velocities, impairing stability.

Our prior work focused on the mechanisms affecting ankle-exoskeleton assisted standing balance, analyzing interactions among age, sex, and stability. Here, we focus on how hardware and software design choices affect stability, using a simple model of an impaired older adult. Previously, we only considered one level of exoskeleton assistance, i.e. an exoskeleton that saturated at $25 \text{ N} \cdot \text{m}$ (providing $50 \text{ N} \cdot \text{m}$ assistance bilaterally) [12]. However, motors used to drive ankle exoskeletons span a range of peak torques, e.g. $20 \text{ N} \cdot \text{m}$ to $50 \text{ N} \cdot \text{m}$ [14]. The ideal amount of assistance is an open question, and experimental studies have shown that metabolic energy consumption during walking can increase with increased exoskeleton torque assistance [15]. Based on results from our prior work, we expect that increased torque

*This work was supported by NIH grants F31-EB032745 and R01AG068102 and NSF grant CPS-1931982

¹D. Raz and N. Ozay are with the University of Michigan Robotics Department, Ann Arbor, MI USA (e-mail: daphraz@umich.edu, necmiye@umich.edu).

²B. R. Umberger is with the University of Michigan School of Kinesiology, Ann Arbor, MI USA (e-mail: umberger@umich.edu).

assistance may also negatively affect standing stability under some conditions.

Furthermore, our prior work used controllers whose gains are determined based on an inverted pendulum model of the standing human, where it is necessary to correctly measure mass and CoM height. We assumed that controller parameters corresponding to mass and CoM height were accurate. Measuring total body mass at a single point in time is simple, but the value relevant for the controller can vary with factors such as clothing (donning a heavy winter coat), load (carrying groceries or wearing a backpack), and natural weight fluctuations. Measuring the true CoM height of a living individual as a percentage of body height, on the other hand, is less routine. A reaction board can be used [16], or the masses and centers of mass of different body segments can be measured, with certain segment measurements being more prone to error than others [17]. These measurements can be difficult to acquire in older adults [18]. Furthermore, CoM height can be variable, even given the same body mass. It can change by several percentage points simply based on posture or arm position [16], and can differ by as much as 15% between males and females [19]. Taken together, these factors can give rise to uncertainty in this value.

Beyond parameter uncertainty and torque assistance, our earlier model assumed that the human could *not* generate torque instantaneously while the exoskeleton itself was modeled as an ideal torque actuator without delay. In reality, most devices use onboard sensors to estimate a relevant state (joint velocity or human ankle torque, e.g.). Such a computation delay, combined with naturally arising communication and physical delays can introduce a net actuation delay, with values such as 0.050 s and 0.124 s reported in the literature [20], [21]. Modeling studies have shown that large exoskeleton delays can hinder stability [22], while experiments have found that exoskeletons must respond faster than the user to improve standing balance [9].

Here we extend our prior work by analyzing the effect of ankle exoskeleton strength, uncertainty in ankle exoskeleton controller parameters, and exoskeleton actuation delay on standing balance in a simple model of a frail, older adult female. We first analyze the effect of three exoskeletons with three different levels of motor strength: a ‘weak’ exoskeleton that provides a low level of assistance, a moderately strong exoskeleton that is optimized to increase static stability, and a ‘strong’ exoskeleton with powerful motors. We then relax our previous assumption that the controller parameters are accurate, and investigate the effect of errors in center of mass location for each level of exoskeleton assistance. Lastly, we assess changes in stability over a range of exoskeleton controller delays.

II. TECHNICAL BACKGROUND

Let

$$\dot{x} = f(x, u), \quad (1)$$

be the dynamics of a generic, nonlinear system. In the context of this paper, these dynamics represent a model of a human

maintaining upright standing balance. Accordingly, state $x \in X \subset \mathbb{R}^n$ consists of the relevant biomechanical states, i.e. joint angles and angular velocities. Depending on the model, set X may incorporate various constraints on the state, such as foot-ground contact constraints.

Input $u \in U \subset \mathbb{R}^m$ is the signal actuating the system, such as joint torques common in biomechanical models. Control signals are denoted $u(\cdot) \in \mathcal{U} = \{\phi : [0, \infty] \rightarrow U\}$. Solutions to this system are functions of time, and we denote them by $\varphi(\cdot; x_0, u(\cdot))$, for initial condition x_0 and control signal $u(\cdot)$.

Let $S \subset X$ be the subset of states corresponding to a stable, upright standing position. Then the *stabilizable region* of (1) is the set of all $x \in X$ from which it is possible to stabilize to S . To compute this region, we use two concepts from control theory: backward reachability and controlled invariance. The backward reachable set of S is the set of all initial conditions $x_0 \in X$ from which it is possible to reach S with in some finite time $T \in [0, \infty)$, or more formally:

Definition 1. Let $S \subset X$ and $T \in [0, \infty)$. Then $\text{BRS}_T(S)$, the *backward reachable set* of S at time T , is

$$\text{BRS}_T(S) := \{x \in X \mid \exists u(\cdot) \in \mathcal{U} \text{ s.t. } \varphi(T; x, u) \in S\}. \quad (2)$$

Set S is often referred to as the *target set*. If S represents quiet standing, then the backward reachable set of S sounds similar to our stabilizable region concept. However, note that there is no guarantee that the system can remain in S once it has reached S . In the context of human standing balance, this means that the backward reachable set may include initial conditions from which the model passes through, or overshoots the quiet standing set. This is undesirable from a control perspective. It is therefore important to guarantee that once the system has reached S , i.e. quiet standing, then it can remain standing. For this, we need to first show that S is *controlled invariant*, meaning that for an initial state $x_0 \in S$, there always exists a controller $u(t)$ such that the system state can be maintained within S :

Definition 2. A set $S \subset X$ is *controlled invariant* for system (1) if, for all $x_0 \in S$, there exists $u(\cdot) \in \mathcal{U}$ such that for all $t \in [0, \infty]$, $\varphi(t; x_0, u(\cdot)) \in S$.

A useful fact is that if S is invariant, then $\text{BRS}_T(S)$ is also invariant for any T [13]. Thus, if the stabilizable region is formulated as the backward reachable set of well-constructed, invariant target set, then it is also guaranteed to exclude ‘overshoot’ states. For a description of our method for constructing controlled invariant target sets, see [12].

III. METHODS

A. Model

We model a standing human as a planar, two-link pendulum (Fig. 1). The first, triangular-shaped link represents the feet as a single segment, and the second represents the rest of the body. The links are connected via a rotational pin-joint at the ankle, and the mass of each link is assumed to be lumped at the CoM. The foot segment is not fixed to the ground, such that foot-ground contact is constrained by the normal

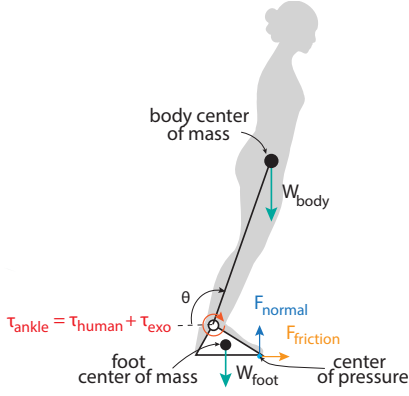


Fig. 1. Free body diagram of the model, adapted from [12]

component of the ground reaction force, horizontal friction force, and location of the center of pressure. A detailed derivation of the model and constraints is in the appendix of [12].

The model is actuated by a torque at the ankle, which is the sum of the torque generated by the human and the ankle exoskeleton. When not specifically analyzing device delay, we assume that the exoskeleton is an ideal torque generator directly producing τ_{exo} , which saturates at some prespecified torque value. Details of the device delay model are in section III-C. We model the human with more constrained torque dynamics, where the human input to the system u is a desired rate of torque development (RTD). While we could also model the human input as an ideal torque actuator, this representation allows us to constrain the speed at which torque can be produced, better reflecting slowed torque dynamics associated with aging [3]. The equations of motion when the foot is in full contact with the ground are

$$\begin{bmatrix} \dot{x}_1 \\ \dot{x}_2 \\ \dot{x}_3 \end{bmatrix} = \begin{bmatrix} -\frac{g}{l_{\text{CoM}}} \cos x_1 - \frac{b}{ml_{\text{CoM}}^2} x_2 + \frac{1}{ml_{\text{CoM}}^2} (x_3 + \tau_{\text{exo}}) \\ u \end{bmatrix}. \quad (3)$$

where m is the body segment mass, l_{CoM} is CoM height, state x_1 is the ankle angle, x_2 is the ankle angular velocity, x_3 is the bilateral human ankle torque, and τ_{exo} is the exoskeleton torque. We enforce the following foot-ground contact constraints (Figure 1):

$$F_{\text{normal}} \geq 0 \quad (C1)$$

$$\text{CoP} \in \text{BoS}, \quad (C2)$$

$$|F_{\text{friction}}| < \mu F_{\text{normal}}, \quad (C3)$$

which we represent as state constraints on the human torque state x_3 (see [12] for derivations and details).

To represent a frail elderly female, we constrain the maximum plantar flexion and dorsiflexion torque values of the human torque state x_3 (MT^{PF} and MT^{DF} , respectively), and the maximum rate of torque development (MRTD) for

the human RTD input u ($MRTD^{\text{PF}}$ and $MRTD^{\text{DF}}$):

$$MT^{\text{PF}} \leq x_3 \leq MT^{\text{DF}} \quad (C4)$$

$$MRTD^{\text{PF}} \leq u \leq MRTD^{\text{DF}}. \quad (C5)$$

We select these values (Table I) based on studies measuring strength in older adults [4], [23], including studies assessing older people who are frequent fallers [24].

TABLE I
MODEL PARAMETERS FOR WEAK OLDER FEMALE, INCLUDING TOTAL MAXIMUM TORQUE (MT) AND MAXIMUM RATE OF TORQUE DEVELOPMENT (MRTD) IN DORSIFLEXION (DF) AND PLANTAR FLEXION (PF) DIRECTIONS

Mass (kg)	Height (m)	MT (N · m)	MRTD (N · m/s)
60.0	1.59	78 (PF) 21 (DF)	303 (PF) 130 (DF)

B. Exoskeleton torque selection and controller design

We assume the bilaterally worn exoskeletons use a state feedback, gravity compensation (GC) control strategy in tandem, as described in [11]:

$$\tau_{\text{exo}}^c(t) = mgl \cos \theta(t), \quad (4)$$

where $\tau_{\text{exo}}^c(t)$ denotes the computed torque value. Because the motors saturate, the effective torque is

$$\tau_{\text{exo}} = \text{sat}_{MT^{\text{exo}}}(\tau_{\text{exo}}^c) = \begin{cases} -MT^{\text{exo}} & \text{if } \tau_{\text{exo}}^c < -MT^{\text{exo}} \\ \tau_{\text{exo}}^c & \text{if } |\tau_{\text{exo}}^c| \leq MT^{\text{exo}} \\ MT^{\text{exo}} & \text{if } \tau_{\text{exo}}^c > MT^{\text{exo}} \end{cases}, \quad (5)$$

where MT^{exo} is the maximum amount of bilateral torque assistance (i.e. double the saturation limit of each exoskeleton). We note that proportional-derivative (PD) control is also popular, however, both [11] and our prior work showed that the effect of PD controllers on feasible standing balance is quite similar, with the extra damping minimally affecting the overall results.

To assess how changes in the exoskeleton motor limit affect the stabilizable region, we consider three different levels of exoskeleton assistance:

- 1) a ‘weakly’ assistive exoskeleton that saturates at 5 N · m ($MT^{\text{exo}} = 10 \text{ N} \cdot \text{m}$ bilateral assistance)
- 2) a ‘moderately’ assistive exoskeleton that saturates at 17 N · m ($MT^{\text{exo}} = 34 \text{ N} \cdot \text{m}$ bilateral assistance)
- 3) a ‘strongly’ assistive exoskeleton saturating at 40 N · m ($MT^{\text{exo}} = 80 \text{ N} \cdot \text{m}$ bilateral assistance)

The ‘strongly’ assistive exoskeleton is similar to other devices described in the literature [14], while the ‘weakly’ assistive exoskeleton is slightly weaker than what is typically reported. We select such a low torque as there is great interest in developing more lightweight devices, and we wish to observe the effect of lower levels of assistance. Finally, we select the motor saturation for the moderately assistive exoskeleton by determining the minimum amount of assistance necessary to maintain static stability with the

CoM above the toe. Denoting the ankle angle corresponding to this CoM position as θ_{toe} , the maximum torque is the difference between the torque required to compensate for gravity and the maximum available plantar flexion torque:

$$MT^{\text{exo}} = mgl \cos \theta_{\text{toe}} - MT^{\text{pf}}. \quad (6)$$

Substituting the model parameters from Table I, we see that the necessary amount of bilateral assistance is approximately $34 \text{ N} \cdot \text{m}$, corresponding to an exoskeleton that saturates at $17 \text{ N} \cdot \text{m}$. This exoskeleton is optimal in the sense that it provides the minimum torque required to maximize the feasible base of support (FBOS). We therefore refer to the ‘moderately’ assistive exoskeleton as ‘FBOS-opt’ for the remainder of the text.

To assess how stability is affected when the l_{CoM} and m parameters are over- or under- estimated, we consider the following gravity compensation controller:

$$\tau_{\text{exo}}^c(t) = (\alpha_m m)g(\alpha_{\text{CoM}} l_{\text{CoM}}) \cos \theta(t), \quad (7)$$

where $\alpha_{\text{CoM}}, \alpha_m$ represent the level of over- or under-estimation for parameters m and l_{CoM} , e.g. $\alpha_{\text{CoM}} = 0.8$ for a 20% underestimated CoM.

C. Approximating exoskeleton delayed state feedback

Our model (3) accounts for slowed torque production dynamics of an impaired older female by limiting the rate at which torque can be generated. To assess how delay in the exoskeleton controller might interact with this age-related deficit, we relax our assumption that the ankle exoskeleton uses a state feedback strategy with access to the current state and assume that the state feedback has a delay δ_{exo} , such that

$$\tau_{\text{exo}}^c(t) = mgl \cos \theta(t - \delta_{\text{exo}}). \quad (8)$$

When substituted into our dynamics (3), we now have a delay differential equation with delayed position feedback. Such equations present serious analytical and computational difficulties, particularly in the context of backward reachability. Thus we approximate the positional feedback using a Taylor series expansion of the delayed position about $\delta_{\text{exo}} = 0$, using the fact that angular velocity is already a state variable:

$$\theta(t - \delta_{\text{exo}}) \approx \theta(t) - \delta_{\text{exo}} \dot{\theta}(t). \quad (9)$$

While this approach is commonly used in biomechanics, such Taylor series approximations are not generally good for preserving the global behavior of the original time-delayed system [25]. However, we consider relatively small delays and note that the delay does not affect the exoskeleton torque outside of the saturation bounds, limiting the worst-case approximation error. We validate via simulation that the error between trajectories of the true delay differential equation and our Taylor series approximation is negligible.

D. Computing and comparing stabilizable regions

Using the method developed in [12], we construct controlled invariant sets representing standing balance, both for the model without an exoskeleton, and for each level of ankle exoskeleton saturation, controller type, and delay level. For

each target set, we compute the backward reachable sets using Hamilton-Jacobi-Bellman (HJB) reachability, which formulates the backward reachable set as the solution to a partial differential equation. The exoskeleton input is a closed loop term that is part of the dynamics (equation (3)). The human RTD input, u , is analytically determined, and is assumed to be the optimal controller for driving the system as close to the target set as possible. This is appropriate for our analysis, as we are interested in analyzing feasible stability, and are not concerned here with other factors that may affect preferred postural control such as effort or smoothness. The HJB approach and its relation to our human-exoskeleton model is detailed in [12].

We first compute a baseline stabilizable region of our model without added exoskeleton assistance. We then compute stabilizable regions for the model wearing each level of exoskeleton assistance (weak, optimal, strong), and calculate the percent change in total area of the region with respect to the baseline. For each assistance level, we then compute the stabilizable region, with the $\alpha_{\text{CoM}} = \pm 20\%$. We select this amount, because CoM location relative to height can differ between men and women by as much as 15% [19] and can further vary due to arm position [16]. This natural variability, combined with the difficulty of estimating the whole-body CoM and the fact that humans are not truly single link pendula, could produce moderately large errors in the l_{CoM} parameter. We again compare the total area of the stabilizable regions with the unassisted baseline.

For our delay analysis, we focus on the FBOS-opt ankle exoskeleton. We select a range of exoskeleton delays by computing the length of time it takes the unassisted model to go from no torque to maximum plantar flexion torque, based on the MRTD, which we call δ_{max} . For the impaired older female model used here, $\delta_{\text{max}} = 0.257 \text{ s}$. We compute the stabilizable region when $\delta_{\text{exo}} = \frac{1}{4}\delta_{\text{max}}, \frac{1}{2}\delta_{\text{max}}, \frac{3}{4}\delta_{\text{max}}$, and δ_{max} . This corresponds to 0.064, 0.129, 0.193, and 0.257 s respectively. While δ_{max} is a large value that may not be seen typically, we include it in our analysis as there is interest in understanding whether there is benefit to an exoskeleton whose delay is ‘synchronized’ with the human [9].

IV. RESULTS

TABLE II
PERCENT CHANGE IN TOTAL AREA OF THE STABILIZABLE REGION OF A FRAIL OLDER FEMALE WEARING AN ANKLE EXOSKELETON WITH RESPECT TO NO-EXOSKELETON BASELINE AT POSITIVE (v^+) AND NEGATIVE (v^-) COM VELOCITIES, FOR THREE DIFFERENT LEVELS OF TORQUE ASSISTANCE AND PARAMETER UNCERTAINTY

v^+	Weak	FBOS-opt	Strong
-20% CoM	10%	17%	-3%
Correct CoM	9%	16%	-3%
+20% CoM	10%	17%	-12%
v^-	Weak	FBOS-opt	Strong
-20% CoM	6%	5%	-39%
Correct CoM	6%	8%	-42%
+20% CoM	6%	4%	-50%

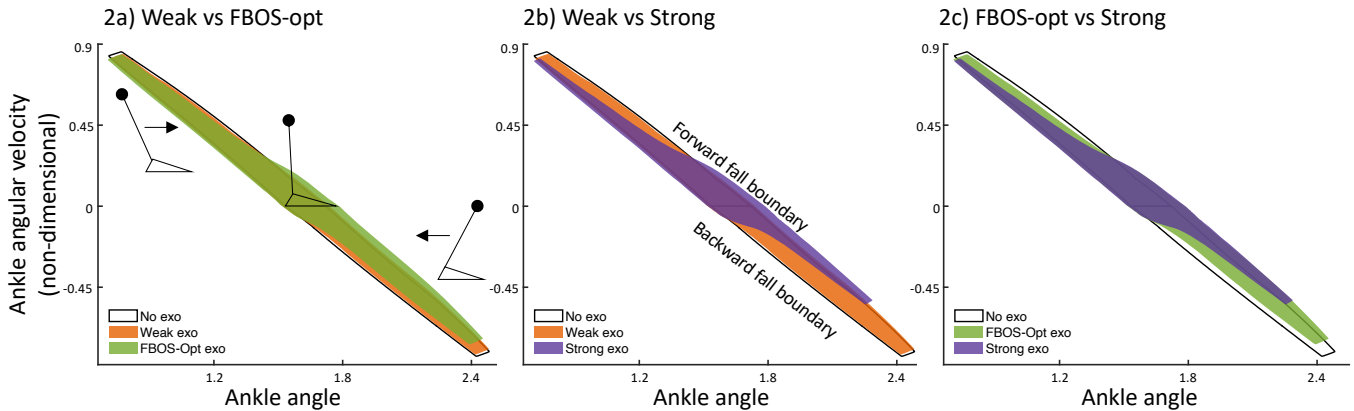


Fig. 2. Pairwise comparison of the stabilizable regions computed for the three different levels of ankle exoskeleton strength using a gravity compensation control strategy. The stick figures in panel 2a indicate body Center of Mass (CoM) positions and velocities (black arrows) relative to the foot segment. The baseline stabilizable region for the frail older female are outlined in black. The weak exoskeleton (orange, panels 2a and 2b) overlaps closely with the baseline region. The FBOS-Opt exoskeleton (green) greatly improves stability at low velocities, as does the strong exoskeleton (purple). However, both torque assistance levels lead to reductions in the stabilizable region at higher magnitude velocities, with the strong exoskeleton hindering stability more than the FBOS-Opt exoskeleton (Panel 2c).

A. Effects of Torque Assistance

The value at which the exoskeleton motor saturates strongly influences the change in stabilizable region area with respect to the no-exoskeleton baseline. The weakly assistive exoskeleton slightly increases the total area of the stabilizable region at both forward and negative velocities (Table II). The FBOS increases slightly (Fig. 2a, note slightly increased width of the stabilizable region at zero angular velocity). The FBOS-Opt exoskeleton increases the stabilizable region area even more, and fully maximizes the FBOS (Fig. 2b). Like the FBOS-Opt exoskeleton, the strongly assistive exoskeleton also fully maximizes the FBOS. Unlike the weak and FBOS-Opt exoskeletons, however, the strongly assistive exoskeleton acts as a major disturbance in some regions of the state space, reducing the overall stabilizable region area by a large amount (Fig. 2c).

Neither the FBOS-Opt exoskeleton nor the strong exoskeleton uniformly increase or reduce stabilizable region area. At low CoM sway velocities, both are equally beneficial and overlap. At higher velocities, both act as a disturbance, tightening the stabilizable region area. This effect is most pronounced along the forward fall/step region at forward velocities and the backward fall/step region at backward velocities (Fig.2).

B. Incorrect CoM Measurement

Underestimation and overestimation of l_{CoM} does not affect stabilizable region area when the weakly assistive exoskeleton is used. At forward velocities the FBOS-opt exoskeleton is also robust to CoM height parameter uncertainty. At negative velocities, however, both an overestimated and underestimated CoM slightly reduce the increase in stabilizable region area that is achievable with the nominal FBOS-opt exoskeleton controller.

The strongly assistive exoskeleton demonstrates the most sensitivity to the l_{CoM} parameter. Overestimating l_{CoM} exacerbates the already large reductions in area caused by the

nominal exoskeleton. Underestimation, on the other hand, has no effect at forward velocities and slightly mitigates the area reduction at negative velocities. Again, we see that changes to the stabilizable region are not uniform. The largest changes relative to the nominal controllers occur at lower velocities (see zoomed-in subpanels in Fig. 3b and 3c).

C. Exoskeleton with delayed state feedback

State feedback delay in the FBOS-Opt exoskeleton controller reduces the increase in total area of the stabilizable region that is achieved by the non-delayed version (Fig. 4). At delay greater than or equal to $\delta_{exo} = .75\delta_{max}$, or 0.193 s, the total area of the stabilizable region begins to decrease with respect to the no-exoskeleton baseline. The reduction occurs mostly at low-velocity nominal conditions (Fig. 5, zoomed-in subpanel).

V. DISCUSSION

We have shown here that the effect of ankle exoskeleton assistance on feasible standing balance in frail older adults depends on the amount of assistance provided, and is also affected by the correctness of controller parameters and device delay. While ankle exoskeletons can both help and hinder standing balance, a stronger exoskeleton is not necessarily better. Based on our analysis, weak ankle exoskeleton assistance may be preferred, because the feasible base of support can be increased slightly, yet the human is better able compensate for the ankle exoskeleton at high velocities where the exoskeleton acts as a disturbance. On the other hand, a stronger exoskeleton increases the stabilizable region at nominal configurations, and can maximize the functional base of support to encompass the entire foot. At a certain point, however, there are diminishing returns. The strong exoskeleton decreases the area of the stabilizable region while the considerably weaker FBOS-Opt exoskeleton significantly increases it. Both levels of assistance hinder stability at large CoM velocities, but the effect is less pronounced for the moderately strong FBOS-Opt exoskeleton.

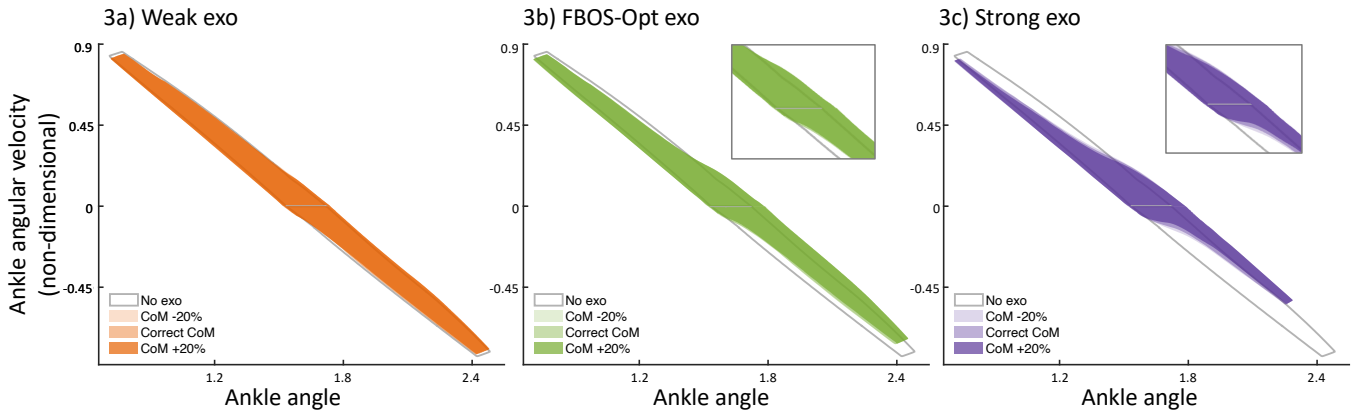


Fig. 3. Stabilizable regions for the (3a) weak, (3b) FBOS-Opt, and (3c) strong exoskeletons using gravity compensation (GC) controllers whose l_{CoM} parameter is correct and $\pm 20\%$ over- and underestimated. The weak GC controller is relatively robust to parameter perturbation as it saturates quickly, while the FBOS-Opt and Strong exoskeleton show increasing sensitivity (zoomed in low-velocity portions of panel 3b and 3c).

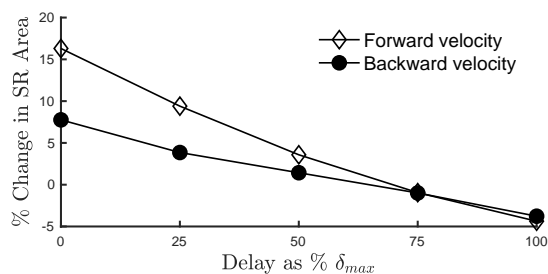


Fig. 4. Exoskeleton actuation delay in FBOS-opt exoskeleton vs % change in stabilizable region area compared to no-exoskeleton baseline. The reductions are separately indicated in the forward velocity portion of the phase plane (clear diamond markers) and backward velocity (filled in black circles). The trend shows exponential decay as delay increases.

The effect of perturbed exoskeleton controller parameters due to incorrect CoM height measurement is relatively moderate. The changes in stabilizable region boundaries are dominated by the maximum torque assistance, MT^{exo} . Indeed, the frail older female model is able to compensate for controller parameter uncertainty in the weakest exoskeleton (Table II and Figure 3). The FBOS-optimal exoskeleton is also fairly robust to this uncertainty at large disturbance magnitudes of $\pm 20\%$. This may be partly because once the motor saturates, the controller with incorrect parameters is equivalent to the nominal controller (i.e. generating a constant maximum torque). At forward velocities, parameter uncertainty in either direction increases the stabilizable region area by approximately 1% more than the nominal exoskeleton. This is likely an artifact of the reachability computation, as overall trends indicate that increasing parameter uncertainty in either direction shrinks the stabilizable region.

For the strong exoskeleton, overestimating the CoM height strongly reduces the stabilizable region area at both forward and backward velocities. Critically, the reduction in stabilizable area occurs at relatively low negative velocities that are close to nominal standing conditions (see zoomed insert in Figure 3c), potentially increasing fall risk. However, *underestimating* CoM height can mitigate the reduction in area. This is because underestimated parameters serve to

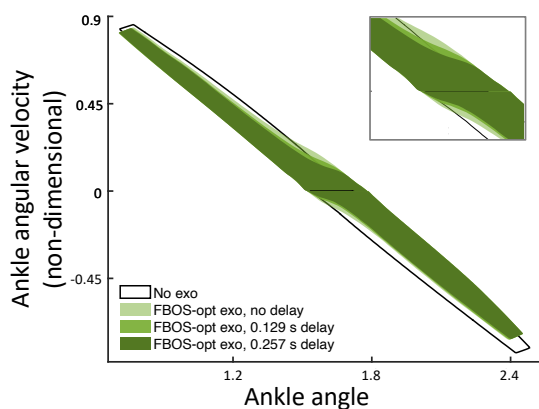


Fig. 5. Stabilizable regions for the FBOS-Opt exoskeleton without delay (light green), $\delta_{\text{exo}} = \frac{1}{2}\delta_{\text{PF}}^{\text{max}}$ (medium green), and $\delta_{\text{exo}} = \delta_{\text{PF}}^{\text{max}}$ (dark green). As the exoskeleton delay increases, the stabilizable region shrinks, particularly at low-velocity conditions.

effectively reduce the total controller gain, meaning that the exoskeleton exerts a lower torque for a given position up until motor saturation.

Compared with CoM height errors, the addition of exoskeleton state feedback delay shows no such beneficial effects. The improvement in total stabilizable region area gets smaller with increasing delay. At $\delta_{\text{exo}} = .75\delta_{\text{max}}$ the delay begins to reduce total stabilizable region area, with total reductions of approximately 5% at both forward and backward CoM velocities. This aligns with experimental results showing no improvement in young adult standing balance when ankle exoskeleton actuation is delayed to coincide with human ankle torque onset [9]. It is reasonable to conjecture that the effect of exoskeleton delay would be even more pronounced in older adults.

In all cases, changes in the stabilizable region are not uniform, particularly for the different variants of the FBOS-opt and strong exoskeleton. In the case of the strong exoskeleton, which sharply reduces overall stabilizable region area, there is a large improvement at low CoM velocities that are closer to typical quiet standing conditions. In contrast,

most of the reduction in area caused by exoskeleton actuation delay occurs at these nominal conditions. This suggests that mitigating actuation delay should be a system design priority.

The non-uniform change in stabilizable region area is in part a result of the interaction between positive work done by the exoskeleton, and negative work done by gravity [12]. In brief, depending on the CoM state, gravity may provide a useful ‘braking’ torque that is reduced or eliminated by the exoskeleton, requiring the user to compensate. Major changes in the stabilizable region area can be explained as a tradeoff between work done by the exoskeleton, gravity, and the strength-limited user [12]. The stronger the exoskeleton, the more critical this tradeoff becomes (Fig. 2). Incorrect controller parameters and delay contribute to this trade-off, further affecting the boundaries of the stabilizable region.

Further reductions in stabilizable region area are a result of the foot-ground interaction constraints and the reduced MT and MRTD of the model, which affects how much the model is able to compensate for the undesirable effects of the exoskeleton. We note that our analysis makes no claim as to how the ankle exoskeleton is resisted by the model, particularly at the level of neuromuscular coordination. Factors such as fatigue and coactivation could further affect feasible stability. We will address this in future work by adding muscle activation dynamics to our model.

Our findings have important implications for ankle exoskeleton design. Reducing actuation delay by mitigating computational delay may be a more critical design criterion than perfectly tuned state-feedback gains. Alongside carefully designed controllers, lightweight exoskeletons with relatively weak motors may potentially provide great benefits. For frail older adults, such devices are preferable as they are more comfortable and present less risk to the user. Our reachability-based method can be used to design standing balance controllers using simple output feedback that is relatively easy to measure, such as ankle joint angles, as opposed to controllers that require more advanced sensing to generate full state feedback of hard-to-measure muscle states. Such simple controllers can be designed to enhance stability without requiring high-capacity motors.

REFERENCES

- [1] S. M. O’Connor and A. D. Kuo, “Direction-dependent control of balance during walking and standing,” *Journal of neurophysiology*, vol. 102, no. 3, pp. 1411–1419, 2009.
- [2] F. B. Horak and L. M. Nashner, “Central programming of postural movements: adaptation to altered support-surface configurations,” *Journal of Neurophysiology*, vol. 55, pp. 1369–1381, Jun 1986.
- [3] D. G. Thelen, A. B. Schultz, N. B. Alexander, and J. A. Ashton-Miller, “Effects of age on rapid ankle torque development,” *The Journals of Gerontology: Series A*, vol. 51A, pp. M226–M232, Sep 1996.
- [4] R. Ema, M. Saito, S. Ohki, H. Takayama, Y. Yamada, and R. Akagi, “Association between rapid force production by the plantar flexors and balance performance in elderly men and women,” *Age*, vol. 38, pp. 475–483, Dec 2016.
- [5] C. J. Hasson, R. E. van Emmerik, and G. E. Caldwell, “Balance decrements are associated with age-related muscle property changes,” *Journal of Applied Biomechanics*, vol. 30, pp. 555–562, Aug 2014.
- [6] T. Cattagni, G. Scaglioni, D. Laroche, J. Van Hoecke, V. Gremaux, and A. Martin, “Ankle muscle strength discriminates fallers from non-fallers,” *Frontiers in Aging Neuroscience*, vol. 6, p. 336, Dec 2014.
- [7] S. N. Robinovitch, F. Feldman, Y. Yang, R. Schonnop, P. M. Leung, T. Sarraf, J. Sims-Gould, and M. Loughin, “Video capture of the circumstances of falls in elderly people residing in long-term care: an observational study,” *The Lancet*, vol. 381, no. 9860, pp. 47–54, 2013.
- [8] A. Kanwar, M. Singh, R. Lennon, K. Ghanta, S. M. McNallan, and V. L. Roger, “Frailty and health-related quality of life among residents of long-term care facilities,” *Journal of aging and health*, vol. 25, no. 5, pp. 792–802, 2013.
- [9] O. N. Beck, M. K. Shepherd, R. Rastogi, G. Martino, L. H. Ting, and G. S. Sawicki, “Exoskeletons need to react faster than physiological responses to improve standing balance,” *Science Robotics*, vol. 8, p. eadf1080, Feb 2023.
- [10] S. Canete, E. B. Wilson, W. G. Wright, and D. A. Jacobs, “The effects of exoskeleton assistance at the ankle on sensory integration during standing balance,” *IEEE Transactions on Neural Systems and Rehabilitation Engineering*, vol. 31, pp. 4428–4438, Nov 2023.
- [11] A. R. Emmens, E. H. F. van Asseldonk, and H. van der Kooij, “Effects of a powered ankle-foot orthosis on perturbed standing balance,” *J. NeuroEngineering and Rehabilitation*, vol. 15, p. 50, Dec 2018.
- [12] D. Raz, V. Joshi, B. R. Umberger, and N. Ozay, “Ankle exoskeletons may hinder standing balance in simple models of older and younger adults,” *IEEE Transactions on Neural Systems and Rehabilitation Engineering*, vol. 33, pp. 1145–1155, 2025.
- [13] D. Raz, L. Yang, B. R. Umberger, and N. Ozay, “Determining the domain of stable human sit-to-stand motions via controlled invariant sets and backward reachability,” in *2023 European Control Conference (ECC)*, pp. 1–7, Jun 2023.
- [14] K. A. Witte, J. Zhang, R. W. Jackson, and S. H. Collins, “Design of two lightweight, high-bandwidth torque-controlled ankle exoskeletons,” in *2015 IEEE International Conference on Robotics and Automation (ICRA)*, pp. 1223–1228, IEEE, 2015.
- [15] R. W. Jackson and S. H. Collins, “An experimental comparison of the relative benefits of work and torque assistance in ankle exoskeletons,” *Journal of applied physiology*, vol. 119, no. 5, pp. 541–557, 2015.
- [16] M. I. Croskey, P. M. Dawson, A. C. Luessen, I. E. Marohn, and H. E. Wright, “The height of the center of gravity in man,” *American Journal of Physiology-Legacy Content*, vol. 61, no. 1, pp. 171–185, 1922.
- [17] I. Kingma, H. M. Toussaint, D. A. Commissaris, M. J. Hoozemans, and M. J. Ober, “Optimizing the determination of the body center of mass,” *Journal of biomechanics*, vol. 28, no. 9, pp. 1137–1142, 1995.
- [18] M. J. Pavol, T. M. Owings, and M. D. Grabiner, “Body segment inertial parameter estimation for the general population of older adults,” *Journal of biomechanics*, vol. 35, no. 5, pp. 707–712, 2002.
- [19] R. L. Summers, S. Platts, J. G. Myers, and T. G. Coleman, “Theoretical analysis of the mechanisms of a gender differentiation in the propensity for orthostatic intolerance after spaceflight,” *Theoretical Biology and Medical Modelling*, vol. 7, pp. 1–8, 2010.
- [20] D. D. Molinaro, K. L. Scherpereel, E. B. Schonhaut, G. Evangelopoulos, M. K. Shepherd, and A. J. Young, “Task-agnostic exoskeleton control via biological joint moment estimation,” *Nature*, vol. 635, no. 8038, pp. 337–344, 2024.
- [21] M. Ding, M. Nagashima, S.-G. Cho, J. Takamatsu, and T. Ogasawara, “Control of walking assist exoskeleton with time-delay based on the prediction of plantar force,” *IEEE Access*, vol. 8, pp. 138642–138651, 2020.
- [22] S. Sharafi and T. K. Uchida, “Stability of human balance during quiet stance with physiological and exoskeleton time delays,” *IEEE Robotics and Automation Letters*, vol. 8, pp. 6211–6218, Aug 2023.
- [23] Y. Kobayashi, Y. Ueyasu, Y. Yamashita, and R. Akagi, “Effects of 4 weeks of explosive-type strength training for the plantar flexors on the rate of torque development and postural stability in elderly individuals,” *International journal of sports medicine*, vol. 37, no. 06, pp. 470–475, 2016.
- [24] D. P. LaRoche, K. A. Cremin, B. Greenleaf, and R. V. Croce, “Rapid torque development in older female fallers and nonfallers: a comparison across lower-extremity muscles,” *Journal of Electromyography and Kinesiology*, vol. 20, pp. 482–488, Jun 2010.
- [25] T. Insperger, “On the approximation of delayed systems by Taylor series expansion,” *Journal of Computational and Nonlinear Dynamics*, vol. 10, no. 2, p. 024503, 2015.